NACA

RESEARCH MEMORANDUM

A TRANSONIC WIND-TUNNEL INVESTIGATION OF AN

UNSWEPT-WING—BODY COMBINATION AT

ANGLES OF ATTACK UP TO 24°

By Bruce B. Estabrooks

Langley Aeronautical Laboratory
Langley Field, Va.

NATIONAL ADVISORY COMMITTEE
FOR AERONAUTICS
WASHINGTON
February 6, 1953

NATIONAL ADVISORY COMMITTEE FOR AERONAUTICS

RESEARCH MEMORANDUM

A TRANSONIC WIND-TUNNEL INVESTIGATION OF AN

UNSWEPT-WING—BODY COMBINATION AT

ANGLES OF ATTACK UP TO 24°

By Bruce B. Estabrooks

SUMMARY

A wing having 0° sweepback of the 0.25-chord line has been inves-
tigated in combination with a body of revolution at Mach numbers from
0.60 to 1.11 for angles of attack up to 24°. During the investigation,
the wing was tested at two longitudinal positions on the body. The
wing had an aspect ratio of 4, taper ratio of 0, and 4-percent-thick
symmetrical airfoil sections parallel to the model plane of symmetry.
The airfoil sections consist of circular arcs with the maximum thick-
ness at the 0.40-chord station.

The development of supersonic flow conditions over the wing at
high subsonic Mach numbers leads to an increase in lift at all angles
of attack and a large reduction in drag at lift coefficients from 0.60
to 1.0. The sudden discontinuities in the pitching-moment curves at a
lift coefficient of approximately 0.60 in the Mach number range from
0.60 to 0.90 were eliminated with further increase in Mach number from
0.95 to 1.11. At Mach numbers from 0.95 to 1.01, however, there were
unstable pitching-moment tendencies above a lift coefficient of 1.0.
The force and moment characteristics were relatively little affected
by the change in longitudinal position of the unswept wing on the body.

INTRODUCTION

As part of a program studying wing-fuselage aerodynamic character-
istics at transonic speeds, an unswept wing has been tested at two
longitudinal positions on a fuselage at Mach numbers from 0.60 to 1.11.
The testing of the wing in the forward position on the fuselage was
limited to an angle of attack of 16° because of load limitations of
the strain-gage balance; therefore, the wing was moved rearward 3 inches
on the fuselage so that the angle-of-attack range of the investigation

could be extended up to 24°. The wing had an aspect ratio of 4, taper ratio of 0, and 4-percent-thick symmetrical airfoil sections and was designed for utilization at supersonic speeds as well as transonic speeds. In a previous investigation, this unswept wing had been tested in conjunction with a systematic series of four bodies at angles of attack from 0° to 7° at Mach numbers from 0.60 to 1.13 (ref. 1).

The results of the present investigation provide an indication of the aerodynamic characteristics of the unswept wing at angles of attack up to 24° in the transonic speed range as well as the effects on the wing-fuselage force and moment characteristics of the longitudinal movement of the wing on the fuselage.

SYMBOLS

A   aspect ratio

b   wing span, in.

$\bar{c}$ wing mean aerodynamic chord, $\dfrac{2}{S}\displaystyle\int_0^{b/2} c^2 dy$, in.

c   local chord parallel to the plane of symmetry, in.

C_D drag coefficient, D/qS

C_{D_0} drag coefficient at zero lift

C_L lift coefficient, L/qS

C_m pitching-moment coefficient, $M_{\bar{c}/4}\big/qS\bar{c}$

D   drag, lb

L   lift, lb

M   free-stream Mach number

$M_{\bar{c}/4}$ pitching moment about $0.25\bar{c}$, in-lb

P_b base pressure coefficient, $\dfrac{p_b - p}{q}$

p_b static pressure at model base, lb/sq ft

p   free-stream static pressure, lb/sq ft

q   free-stream dynamic pressure, $\rho V^2/2$, lb/sq ft

S   wing-plan-form area to center line of model, sq ft

V   free-stream velocity, ft/sec

α angle of attack of fuselage center line, deg

ρ free-stream density, slugs/cu ft

APPARATUS

Tunnel

The investigation was conducted in the Langley 8-foot transonic tunnel which is a dodecagonal slotted-throat, single-return wind tunnel designed to obtain aerodynamic data through the speed of sound without the usual effects of choking and blockage. A complete description of the wind-tunnel test section may be found in reference 2 and complete calibrations of the tunnel are presented in reference 3.

Configurations

The wing of the wing-fuselage configuration had 0° sweepback of the 0.25-chord line, an aspect ratio of 4, and a taper ratio of 0. The airfoil sections parallel to the model plane of symmetry were 4-percent-thick symmetrical sections made up of circular arcs with the maximum thickness at the 0.40-chord station. The unswept wing was tested at 0° incidence in a midwing position at two longitudinal locations on a body of revolution. The two longitudinal locations of the wing on the body had the wing 0.25-chord line located at the 0.616- and 0.686-fuselage stations (fig. 1). The body of revolution was cylindrical rearward of the 0.523-fuselage station and the ordinates defining the forebody and cylindrical afterbody are presented in table I. The fineness ratio of the body was 11.46 and the ratio of the wing area to the fuselage frontal area was 13.03. The wing-body combination with the wing in the forward position was the same as that used in the investigation described in reference 4. It should be noted that this body is somewhat larger than the similar body of reference 1.

Model Support System

A three-component internal electrical strain-gage balance was attached to the body of the wing-fuselage configuration at its forward end. The rear portion of the balance was comprised of a sting that was cylindrical from the model base rearward with a diameter slightly less than that of the body. (Note fig. 1).

The support system and the angle-of-attack mechanism are described in reference 5. In order to keep the model reasonably close to the tunnel axis when the angle of attack was varied from $0°$ to $24°$, various couplings were installed ahead of the pivot point of the sting. Consequently, at $0°$ angle of attack, the model was offset from the tunnel axis slightly.

Measurements and Accuracy

The flow in the region of the test section occupied by the model was satisfactorily uniform at all test Mach numbers. Deviations from the average free-stream Mach number did not exceed 0.003 at subsonic speeds, and not more than 0.010 with further increase in Mach number to 1.11 (ref. 3).

The lift and drag coefficients are based on the wing area of 1 square foot. The pitching-moment coefficients are based on the wing area of 1 square foot, the wing mean aerodynamic chord of 8.00 inches, and are taken about the 0.25-chord position of the wing mean aerodynamic chord of the respective configurations. From the static calibrations and reproducibility of the data, the measured coefficients at an angle-of-attack range of $0°$ to $24°$ were estimated to be accurate to within the following limits:

	Subsonic speeds	Transonic speeds
C_L	± 0.016	± 0.008
C_D	$\pm 0.002(\alpha = 0°)$ to $\pm 0.008(\alpha = 24°)$	$\pm 0.001(\alpha = 0°)$ to $\pm 0.004(\alpha = 24°)$
C_m	± 0.002	± 0.002

The limits of the accuracies presented are judged to be the maximum deviations and, in general, the accuracy of the measured coefficients may be expected to be better. The base pressures were determined as the average of readings from four static-pressure orifices located at $90°$ increments around the sting in the plane of the model base. The base pressure coefficients were estimated to be accurate within ± 0.003.

The angle of attack of the model was measured by a pendulum-type accelerometer calibrated against angle of attack. The accelerometer, located in the nose of the model, in conjunction with the remotely controlled angle-of-attack changing mechanism allowed the model angle of attack to be set to within an estimated ±0.1°.

The axially slotted test section minimized boundary interference due to solid blockage (ref. 6) and the effects of wake blockage were similarly reduced. For the range of Mach numbers above 1.0, however, shocks and expansions from the model nose were reflected back to the surface of the model by the test-section boundary. On the basis of reference 7, it may be assumed that the effects of the boundary-reflected disturbances on the aerodynamic characteristics were small.

The average Reynolds number, based on the mean aerodynamic chord of 8.00 inches, varied from 2.28×10^6 to 2.68×10^6 in the Mach number range of 0.60 to 1.11.

RESULTS

The results of this transonic investigation present the wing-fuselage force and moment characteristics of the unswept wing tested in two longitudinal positions on the fuselage. The drag coefficients presented herein have been adjusted to conditions where the base pressure is considered equal to the free-stream static pressure. The base pressure coefficients include the tare effect of the sting. The base pressure coefficients for the wing-fuselage combination are presented in figure 2.

The lift, pitching-moment, and drag characteristics of the wing-fuselage combinations are presented in figures 3 to 5, 6 and 7, and 8 to 10, respectively. The maximum lift-drag ratios are shown in figure 11.

In order to facilitate presentation of the data, staggered scales have been used in several of the figures and care should be taken in selecting the zero axis for each curve. Data for the fuselage alone at angles of attack up to approximately 7° at Mach numbers from 0.80 to 1.10 are presented in reference 8.

DISCUSSION

Lift Characteristics

The variation of lift coefficient with angle of attack (fig. 3) indicates that the lift curves are essentially the same for the wing at the two longitudinal positions on the body. This was to be expected since the wing at both longitudinal positions was located on the cylindrical portion of the body, and, consequently, the upflow over the body affecting the wing was approximately the same.

The lift curves of the wing-fuselage combinations (fig. 3) were nearly linear up to an angle of attack of approximately 7° throughout the Mach number range. At Mach numbers from 0.60 to 0.90, partial stall conditions existed over the wing when the angle of attack was increased beyond 7°. With increase in Mach number to 0.95, the break in the lift curve was delayed to an angle of attack of approximately 16°, where the wing experienced relatively large reductions in lift. With further increase in Mach number from 0.98 to 1.01, an indication of maximum lift occurred at approximately 22° angle of attack. At Mach numbers from 1.03 to 1.11, within the limits of the available data, no rapid changes in the lift curves were noted.

The delay and subsequent elimination of the partial stall conditions over the wing were associated with the reattachment of the flow over the forward part of the upper surface of the wing when local supersonic velocities were attained. This type of flow phenomena has been discussed in reference 9.

The lift-curve slopes of the wing-fuselage combinations averaged over the angle-of-attack range from 0° to 7° are presented in figure 4. Since the longitudinal movement of the wing on the fuselage had little effect on the lift characteristics, the lift-curve slopes of figure 4 represent both configurations. The wing-fuselage combinations experienced a gradual increase of lift-curve slope as the Mach number was increased to about 1.00, followed by a slight decrease with further increase in Mach number to 1.11.

The variation with Mach number of the lift coefficients for the wing-fuselage combination with the wing at the rearward position on the fuselage is presented in figure 5. At angles of attack up to 7°, this configuration experienced a gradual increase in lift coefficient with increase in Mach number to about 0.98, followed by a slight decrease with increase in Mach number to 1.11. At angles of attack from 10° to 24°, the wing-fuselage combination experienced an abrupt increase in lift in the Mach number range of 0.85 to 0.98 as supersonic flow conditions developed over the wing.

Pitching Moment

The variation with lift coefficient of the pitching-moment coefficients is presented in figure 6. The unswept wing of the present investigation experienced abrupt pitching-moment breaks that were unusual for unswept wings (refs. 10 and 11) and might possibly be due to the airfoil-section characteristics. The wing experienced abrupt rearward (stabilizing) shifts of the aerodynamic center at lift coefficients varying from approximately 0.50 to 0.70 at Mach numbers from 0.60 to 0.90. These abrupt shifts of the aerodynamic center were associated with the breaks noted in the discussion of the lift curves (fig. 3) and were due to the rapid expansion of a region of separated flow over the wing. With further increase in Mach number to 1.11, improved stability characteristics were indicated for the lift-coefficient range from 0 to approximately 1.0. These improved stability characteristics were associated with the normal rearward progression of the center of pressure caused by the development of supersonic flow conditions over the wing. However, severe unstable tendencies are indicated at lift coefficients above a value of approximately 1.0 for Mach numbers from 0.95 to 1.01. At Mach numbers from 1.03 to 1.11, the trends of the pitching-moment curves at lift coefficients above 1.0 cannot be defined because of the load limitations of the strain-gage balance.

The variation with Mach number of the static-longitudinal-stability parameter $\partial C_m/\partial C_L$ presented in figure 7 indicates that the longitudinal movement of the wing on the fuselage had little influence on the stability characteristics. At lift coefficients of 0 and 0.4, the two wing-fuselage configurations experienced similar variations of $\partial C_m/\partial C_L$ with increase in Mach number through the transonic speed range. The value of $\partial C_m/\partial C_L$ decreased approximately 0.15 with increase in Mach number from 0.80 to 1.11.

Drag Characteristics

The variation of drag coefficient with lift coefficient at constant Mach numbers presented in figure 8 indicates that at low lift coefficients the longitudinal movement of the wing on the fuselage had little effect on the drag characteristics. At lift coefficients from 0.6 to 1.0, the wing experienced large reductions in drag with increase in Mach number to approximately 0.98 (fig. 9). For example, at a lift coefficient of 0.8, the drag was decreased approximately 50 percent with increase in Mach number to 0.98. These reductions in drag were associated with the development of supersonic flow conditions over the wing and subsequent elimination of separated flow over the forward part of the wing associated with the increase in Mach number to 0.98, which contributed to the increase in lift noted in the discussion of figure 5. The drag increase experienced by the wing-fuselage combination at the

higher lift coefficients $(C_L = 0.6$ to $1.0)$ as the Mach number was
increased from 0.98 to 1.11 was as expected from noting the variation
of lift coefficient with Mach number (fig. 5).

The variation of drag coefficient due to lift against lift coef-
ficient squared is shown for several Mach numbers in figure 10 along
with the minimum elliptical induced drag $C_L^2/\pi A$ and the theoretical
drag due to lift with no leading-edge suction $C_L \tan \alpha$. The results
indicate that the wing experienced relatively little leading-edge suc-
tion throughout the lift-coefficient range at all the Mach numbers
presented.

Lift-Drag Ratio

The variation with Mach number of the maximum lift-drag ratio for
the two wing-fuselage configurations is presented in figure 11. The
configurations with the wing located at two longitudinal positions on
the fuselage experienced almost the same variations of lift-drag ratio
through the transonic speed range. The maximum lift-drag ratio decreased
rapidly from 12 to 9.5 with increase in Mach number from 0.90 to 0.95
and then decreased gradually to a value of 7.8 with further increase
in Mach number to 1.11.

CONCLUSIONS

The following conclusions may be reached from a transonic wind-
tunnel investigation to determine the aerodynamic characteristics of
an unswept wing located at two longitudinal positions on a fuselage
at angles of attack up to 24°:

1. The development of supersonic flow conditions over the wing at
transonic Mach numbers led to an increase in lift at all angles of
attack and contributed to large reductions in drag at lift coefficients
from 0.60 to 1.0.

2. The sudden discontinuities in the pitching-moment curves at a
lift coefficient of approximately 0.60 in the Mach number range from
0.60 to 0.90 were eliminated with further increase in Mach number from
0.95 to 1.11. However, at Mach numbers from 0.95 to 1.01, there were
unstable pitching-moment tendencies above a lift coefficient of 1.0.
At Mach numbers from 1.03 to 1.11, the data were insufficient to estab-
lish definite trends above a lift coefficient of 1.0.

3. The drag due to lift of the wing was relatively little affected
by leading-edge suction throughout the lift-coefficient range at all
Mach numbers.

4. The longitudinal position of the wing on the cylindrical portion of the fuselage had little influence on the force and moment characteristics of the wing-fuselage combination in the transonic speed range.

Langley Aeronautical Laboratory,
    National Advisory Committee for Aeronautics,
        Langley Field, Va.

REFERENCES

1. Estabrooks, Bruce B.: Transonic Wind-Tunnel Investigation of an Unswept Wing in Combination With a Systematic Series of Four Bodies. NACA RM L52K12a, 1952.

2. Wright, Ray H., and Ritchie, Virgil S.: Characteristics of a Transonic Test Section With Various Slot Shapes in the Langley 8-Foot High-Speed Tunnel. NACA RM L51H10, 1951.

3. Ritchie, Virgil S., and Pearson, Albin O.: Calibration of the Slotted Test Section of the Langley 8-Foot Transonic Tunnel and Preliminary Experimental Investigation of Boundary-Reflected Disturbances. NACA RM L51K14, 1952.

4. Whitcomb, Richard T.: A Study of the Zero-Lift Drag-Rise Character-istics of Wing-Body Combinations Near the Speed of Sound. NACA RM L52H08, 1952.

5. Osborne, Robert S.: A Transonic-Wing Investigation in the Langley 8-Foot High-Speed Tunnel at High Subsonic Mach Numbers and at a Mach Number of 1.2. Wing-Fuselage Configuration Having a Wing of 45° Sweepback, Aspect Ratio 4, Taper Ratio 0.6, and NACA 65A006 Airfoil Section. NACA RM L50H08, 1950.

6. Wright, Ray H., and Ward, Vernon J.: NACA Transonic Wind-Tunnel Test Sections. NACA RM L8J06, 1948.

7. Osborne, Robert S., and Mugler, John P., Jr.: Aerodynamic Charac-teristics of a 45° Sweptback Wing-Fuselage Combination and the Fuselage Alone Obtained in the Langley 8-Foot Transonic Tunnel. NACA RM L52E14, 1952.

8. Williams, Claude V.: A Transonic Wind-Tunnel Investigation of the Effects of Body Indentation, as Specified by the Transonic Drag-Rise Rule, on the Aerodynamic Characteristics and Flow Phenomena of an Unswept-Wing–Body Combination. NACA RM L52L23, 1953.

9. Lindsey, W. F., Daley, Bernard N., and Humphreys, Milton D.: The Flow and Force Characteristics of Supersonic Airfoils at High Subsonic Speeds. NACA TN 1211, 1947.

10. Heitmeyer, John C.: Lift, Drag, and Pitching Moment of Low-Aspect-Ratio Wings at Subsonic and Supersonic Speeds - Plane Tapered Wing of Aspect Ratio 3.1 With 3-Percent-Thick Rounded-Nose Section. NACA RM A52D23, 1952.

11. Reese, David E., and Phelps, E. Ray: Lift, Drag, and Pitching Moment
     of Low-Aspect-Ratio Wings at Subsonic and Supersonic Speeds - Plane
     Tapered Wing of Aspect Ratio 3.1 With 3-Percent-Thick, Biconvex
     Section. NACA RM A50K28, 1951.

TABLE I

BODY ORDINATES

All dimensions are in inches

Station	Radius
0	0
.225	.104
.338	.134
.563	.193
1.125	.325
2.250	.542
3.375	.726
4.500	.887
6.750	1.167
9.000	1.391
11.250	1.559
13.500	1.683
15.750	1.770
18.000	1.828
20.250	1.864
22.500	1.875
43.000	1.875

Wing Details

Airfoil section parallel to plane of symmetry	Circular-arc, $(t/c)_{max}$ at 0.4c, 4-percent-thick, symmetrical
Area, sq ft	1
Aspect ratio	4
Taper ratio	0
Sweepback of quarter-chord line, deg	0
Incidence, deg	0
Dihedral, deg	0
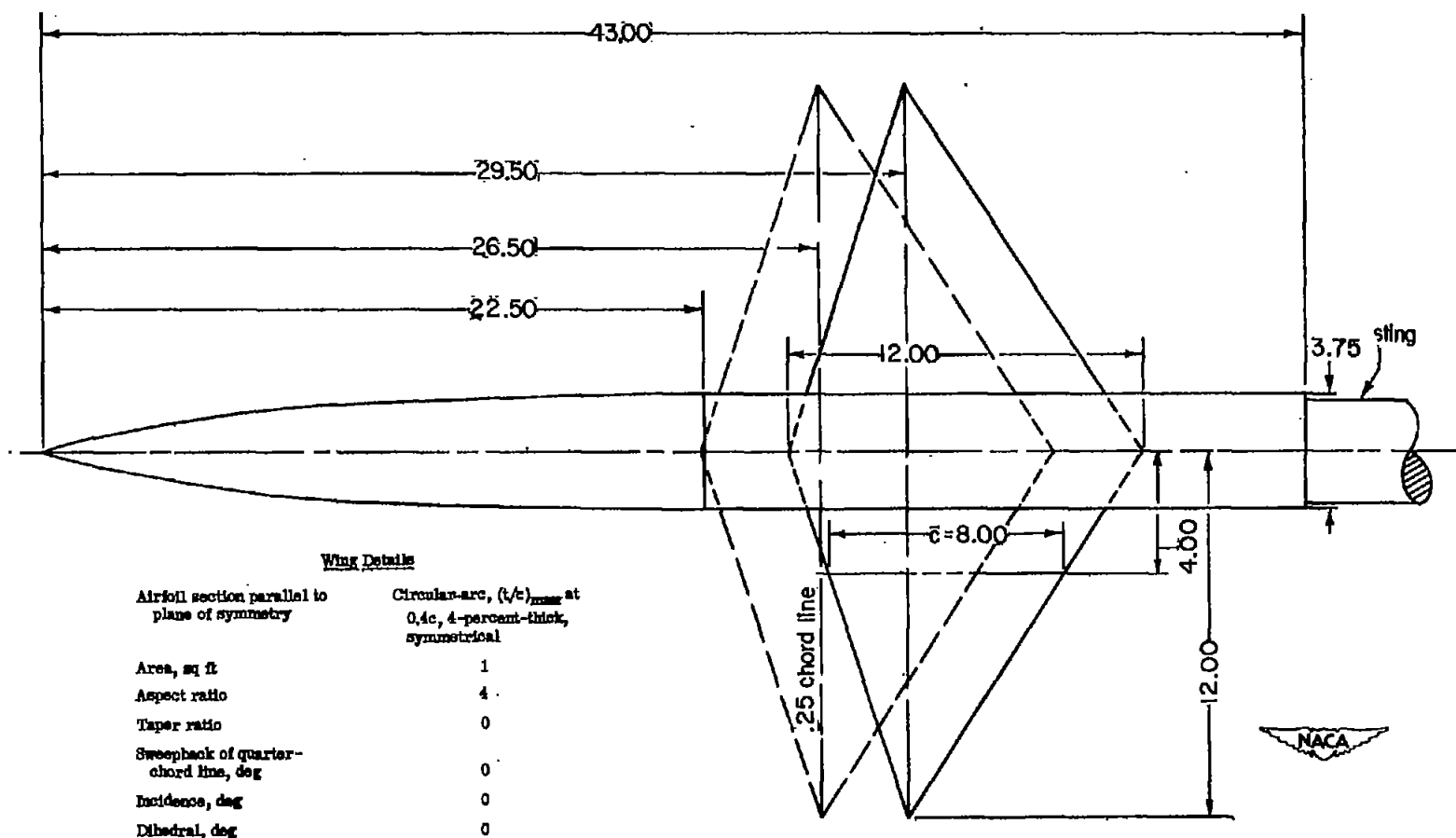
Figure 1.- Details of the wing-fuselage combinations investigated in the slotted test section of the Langley 8-foot transonic tunnel. All dimensions are in inches.
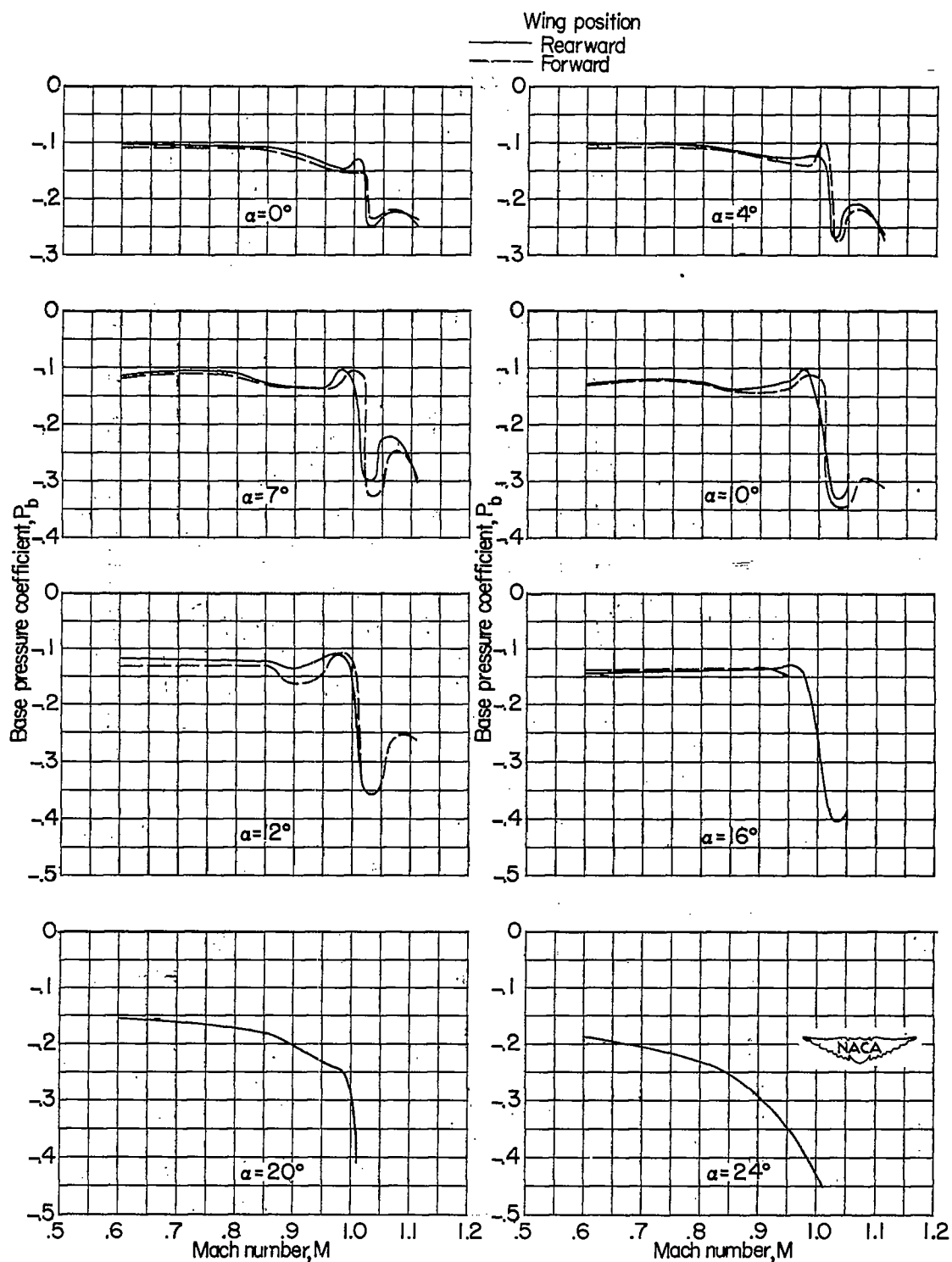
Figure 2.- Variation with Mach number of the base pressure coefficient
for the unswept wing–fuselage configurations.
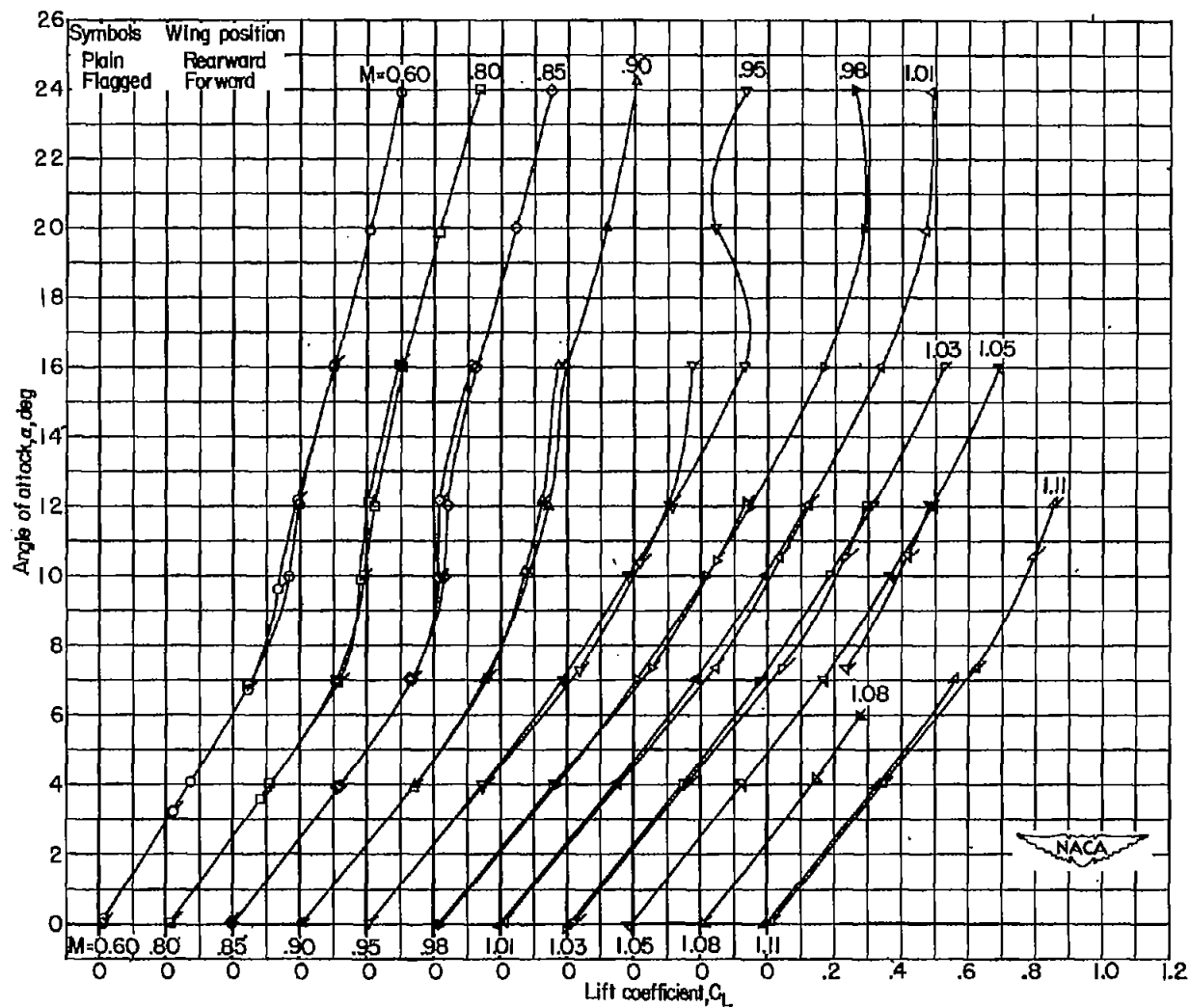
Figure 3.- Variation with lift coefficient of the angle of attack for
the unswept-wing–fuselage combinations.
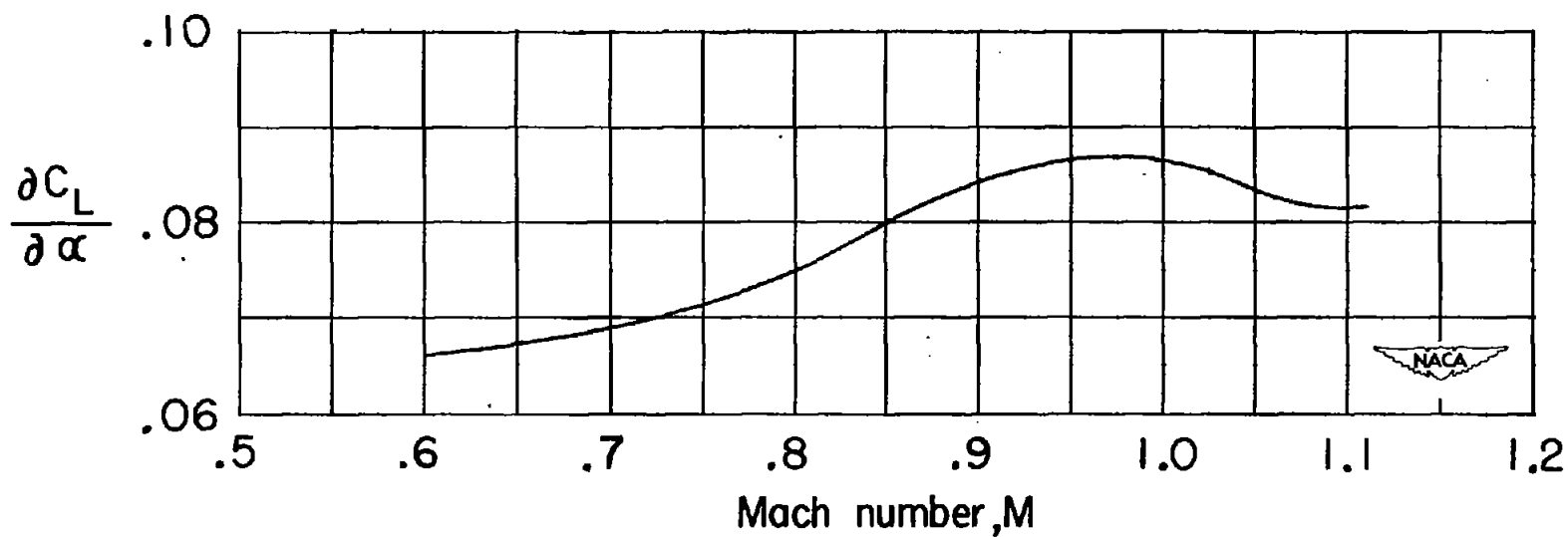
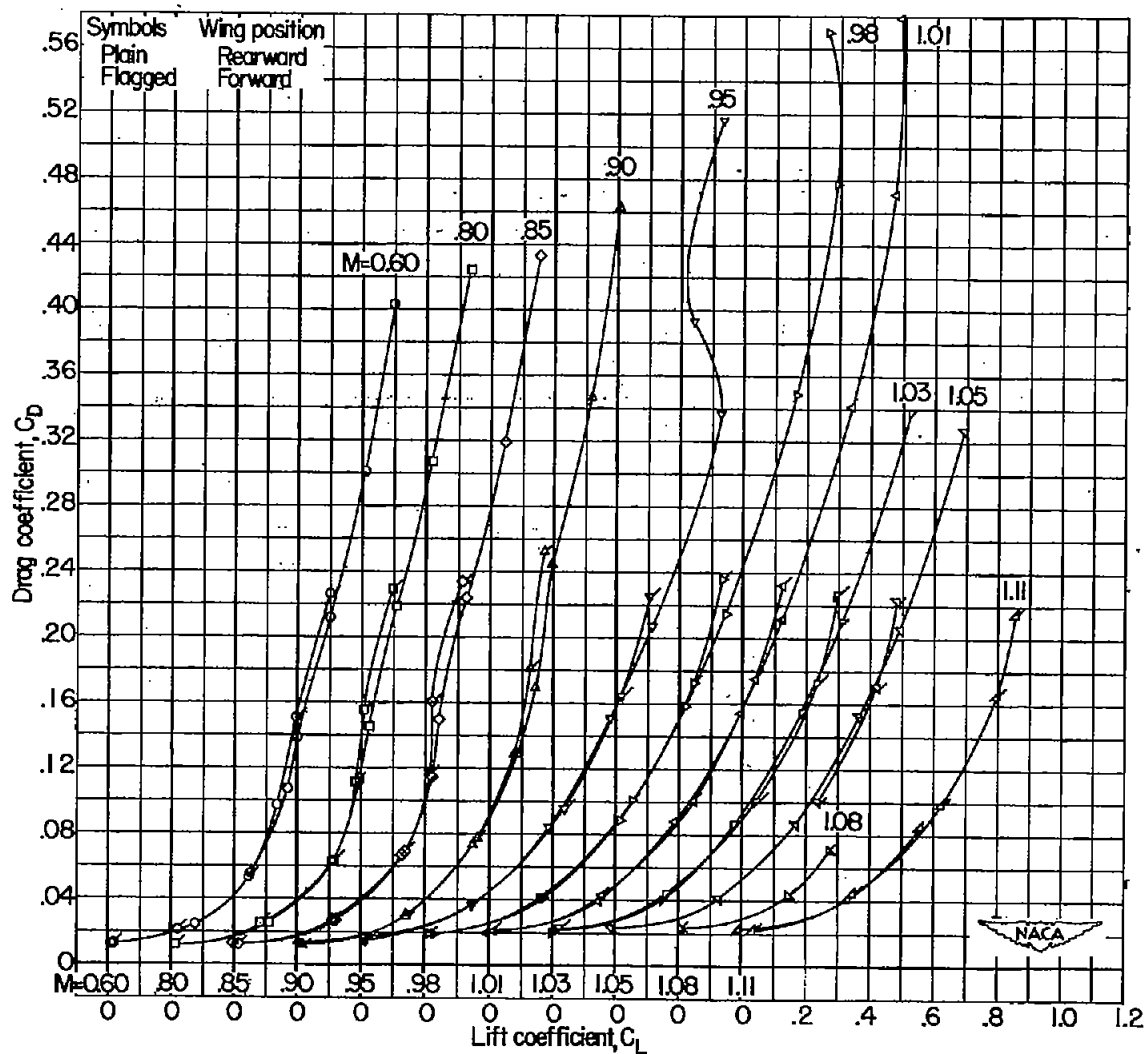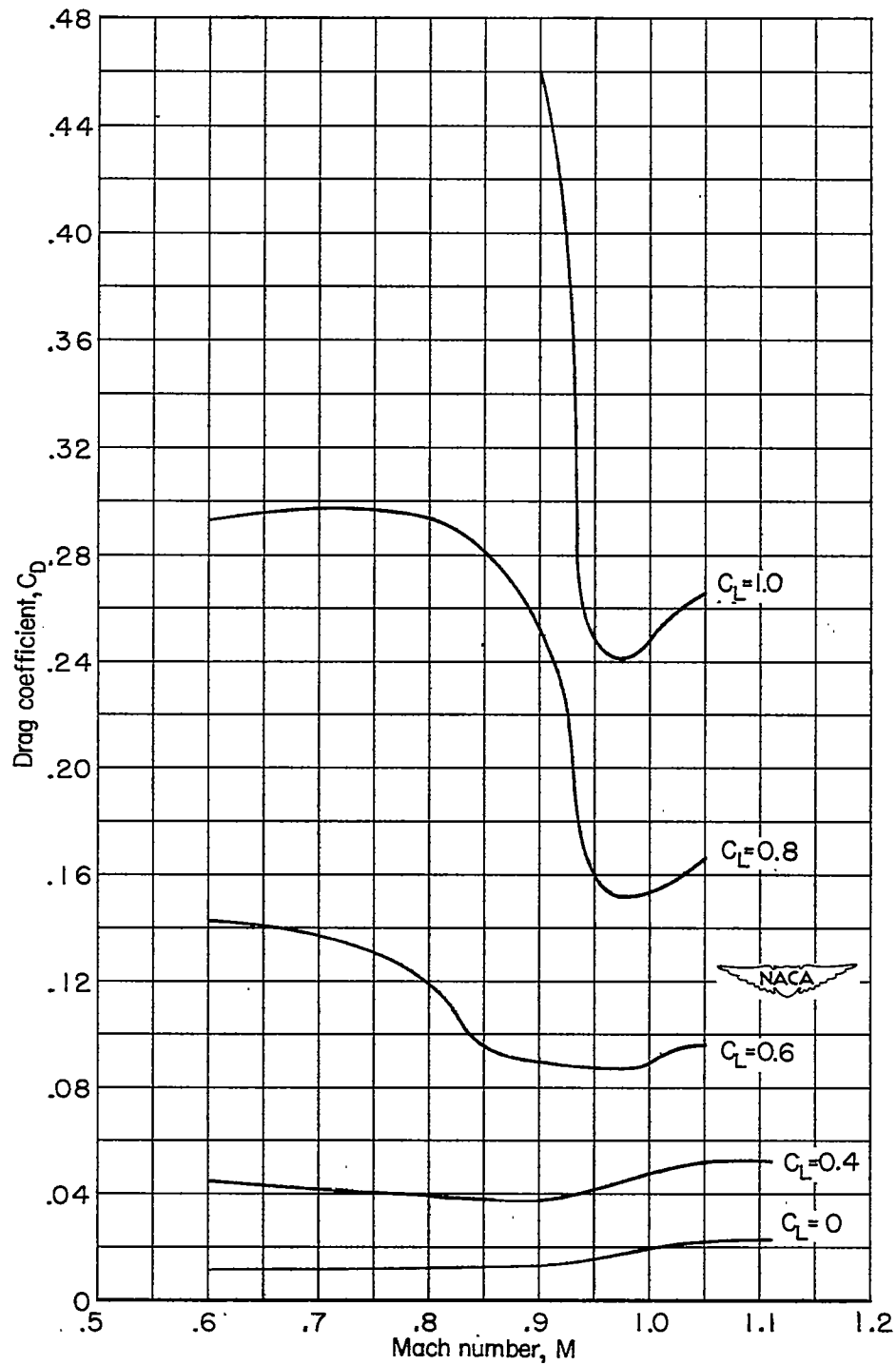Figure 4.- Variation with Mach number of the mean lift-curve slopes at low lift coefficients for the wing-fuselage combinations.
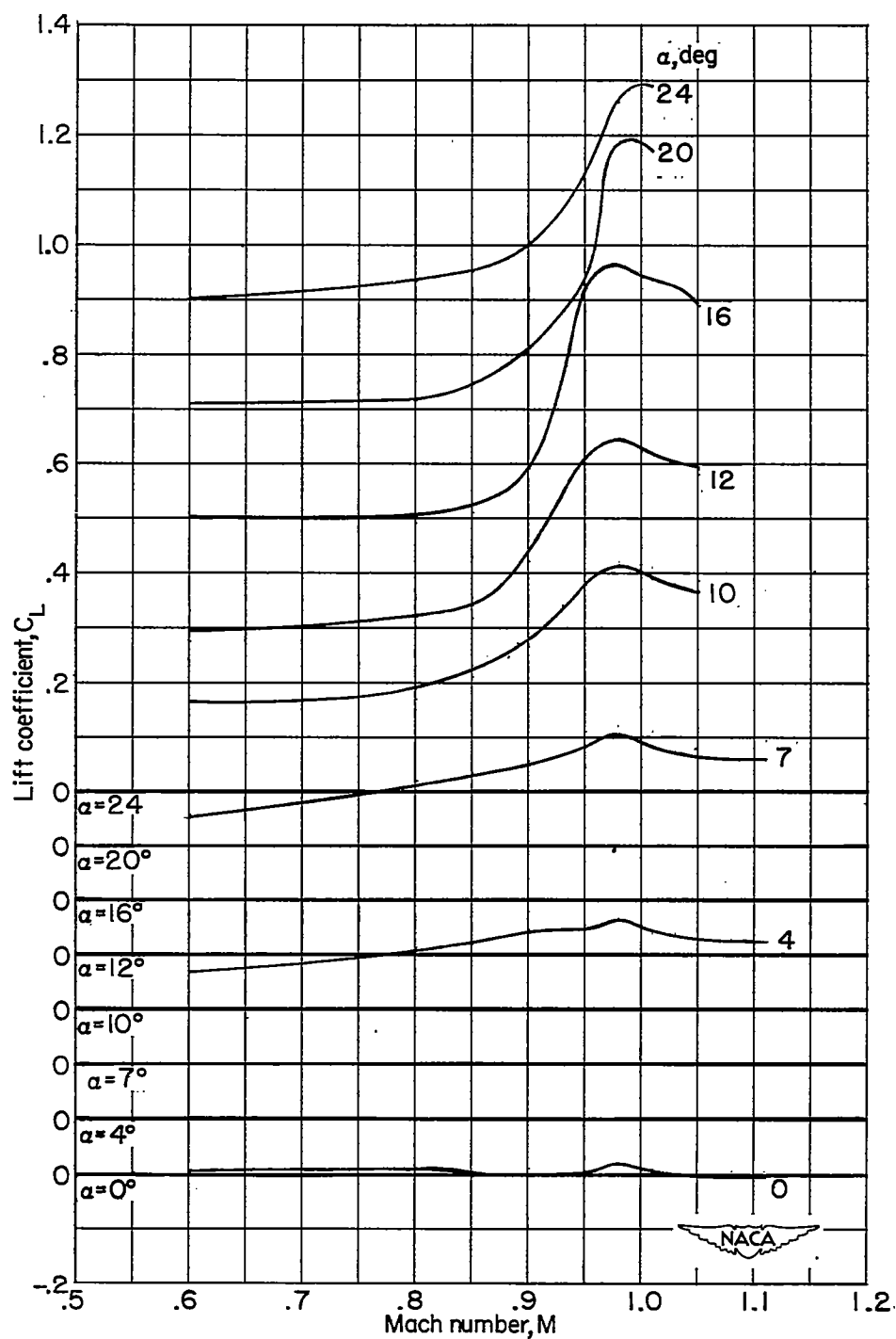
Figure 5.- Variation with Mach number of the lift coefficient at several angles of attack for the unswept wing in the rearward position on the body.

Symbols   Wing position
Plain   Rearward
Flagged   Forward
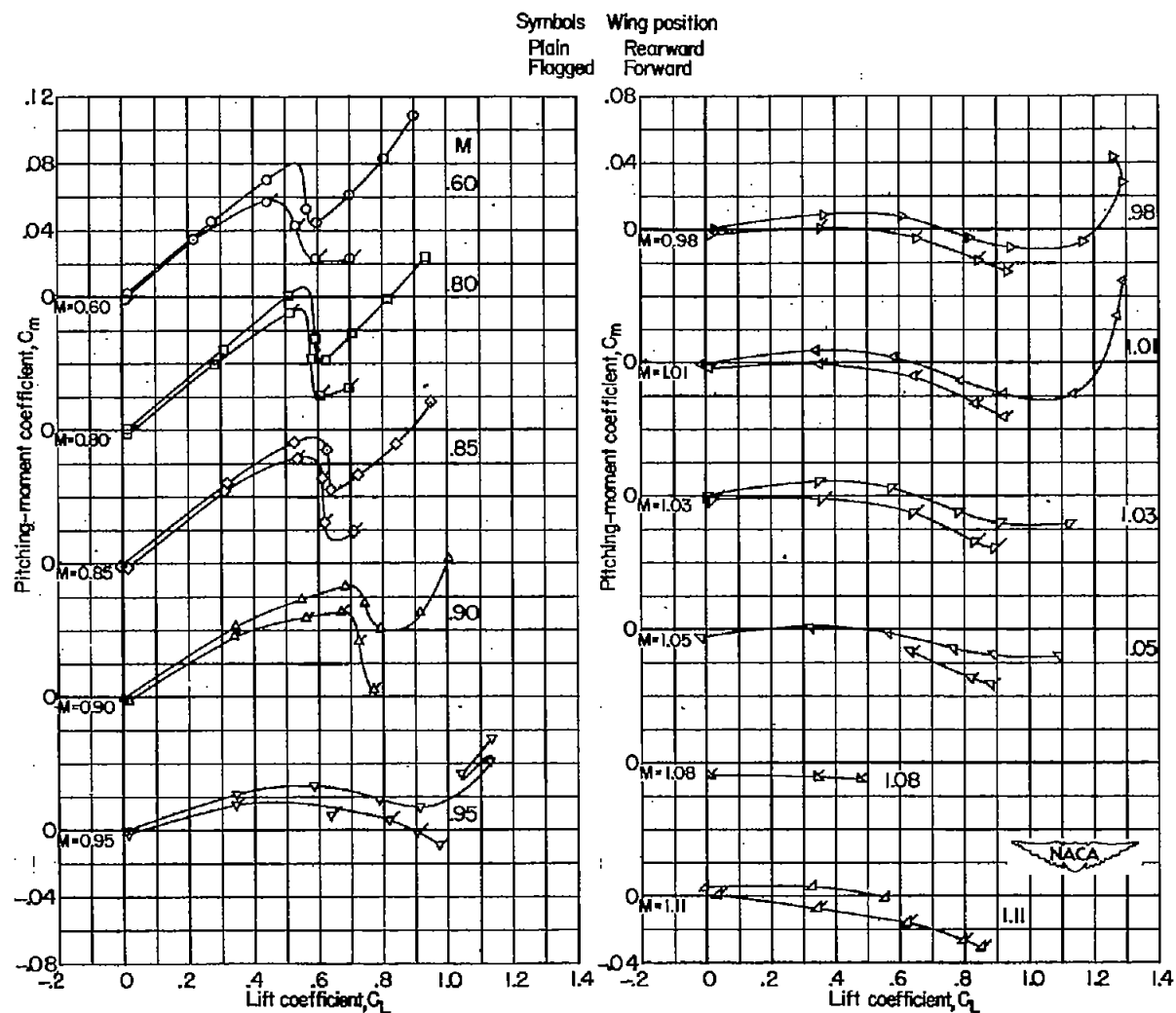
Figure 6.- Variation with lift coefficient of the pitching-moment coefficients for the unswept-wing–fuselage combinations.
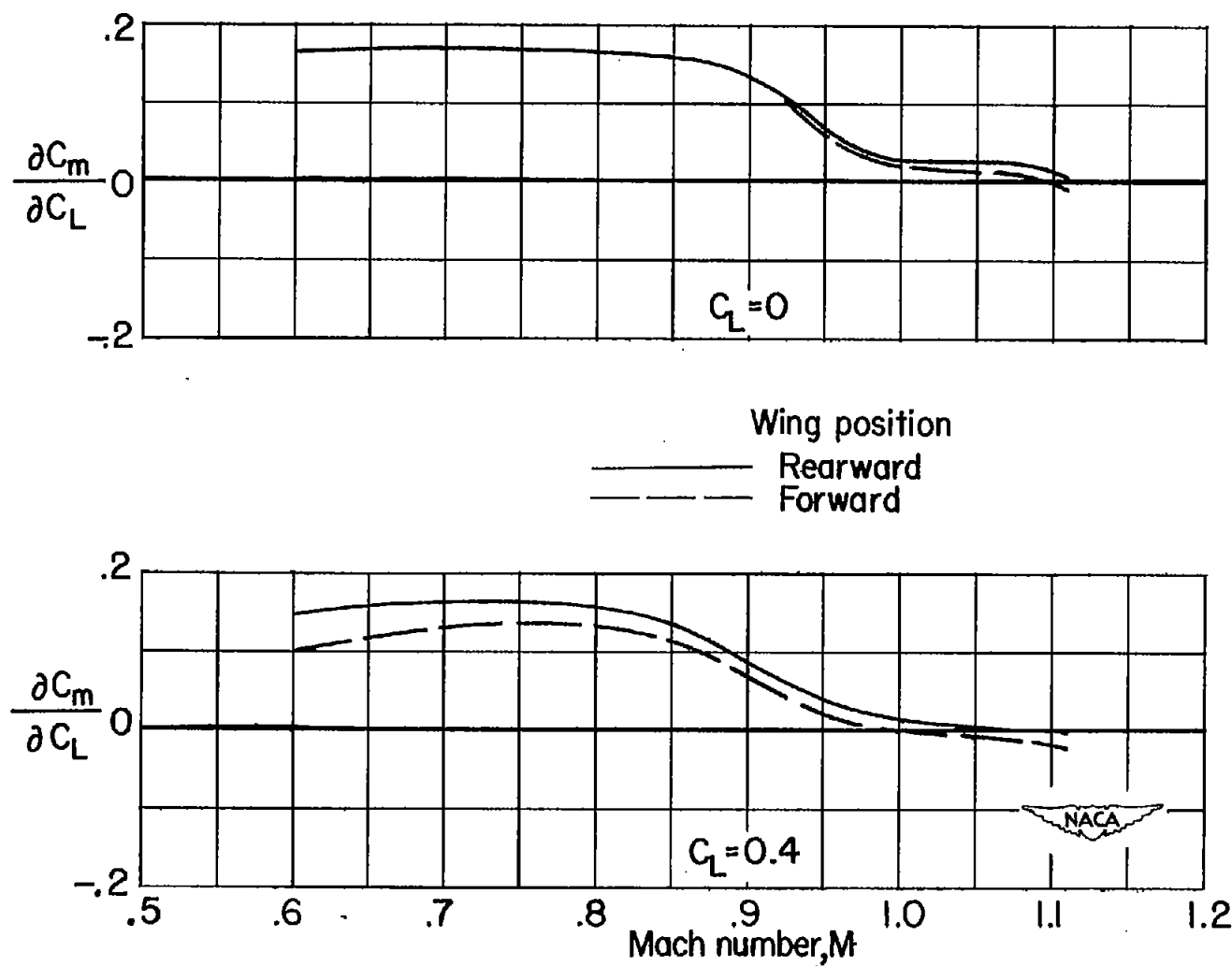
Figure 7.- Variation with Mach number of the static-longitudinal-stability parameter $\partial C_m / \partial C_L$ for the unswept-wing–fuselage combinations.

Figure 8.- Variation with lift coefficient of the drag coefficients for
the unswept-wing-fuselage combinations.

Figure 9.- Variation with Mach number of the drag coefficient at several lift coefficients of the unswept wing in the rearward position on the body.
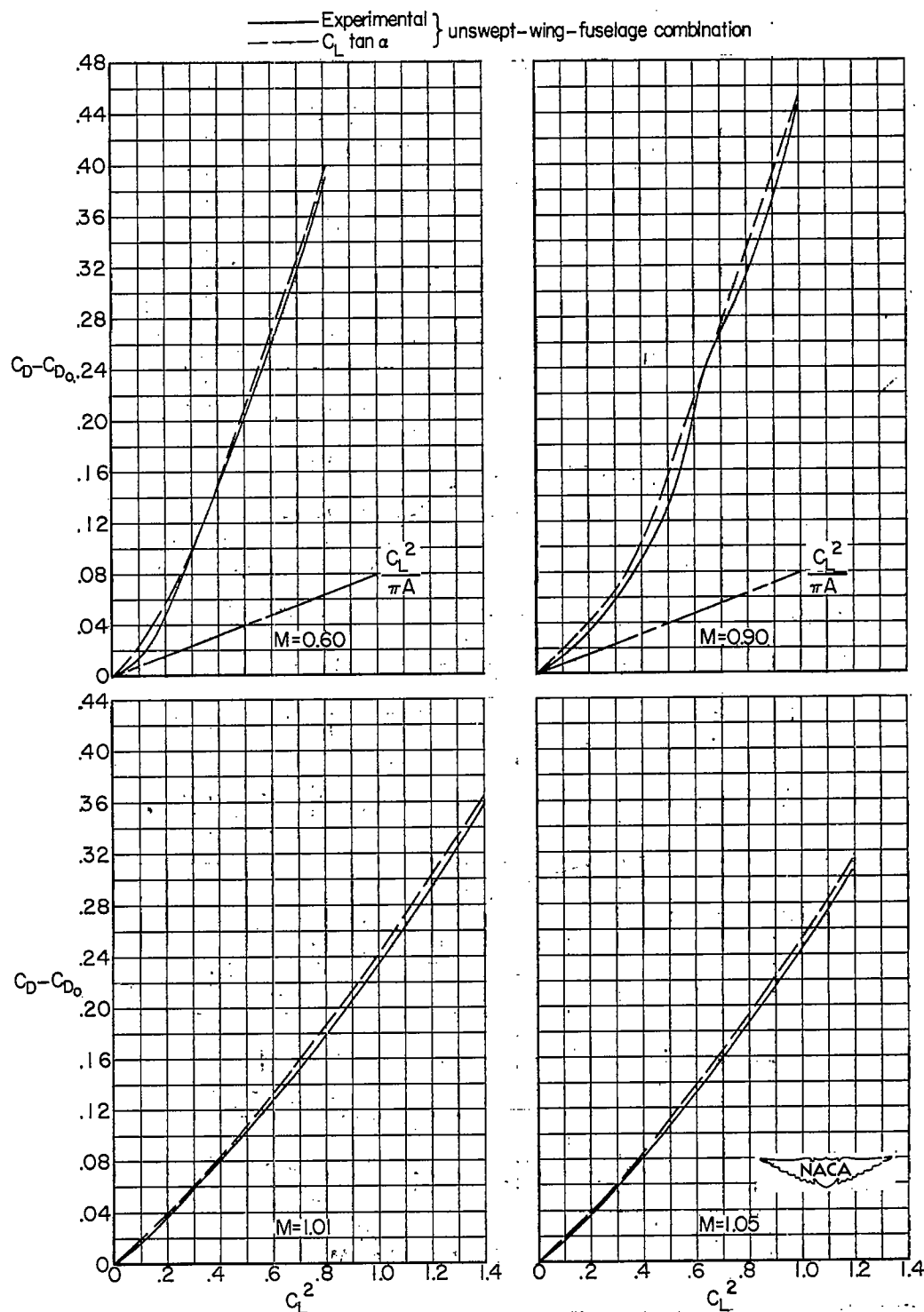
Figure 10.- The variation of drag coefficient due to lift with lift coefficient squared for unswept-wing-fuselage combinations.
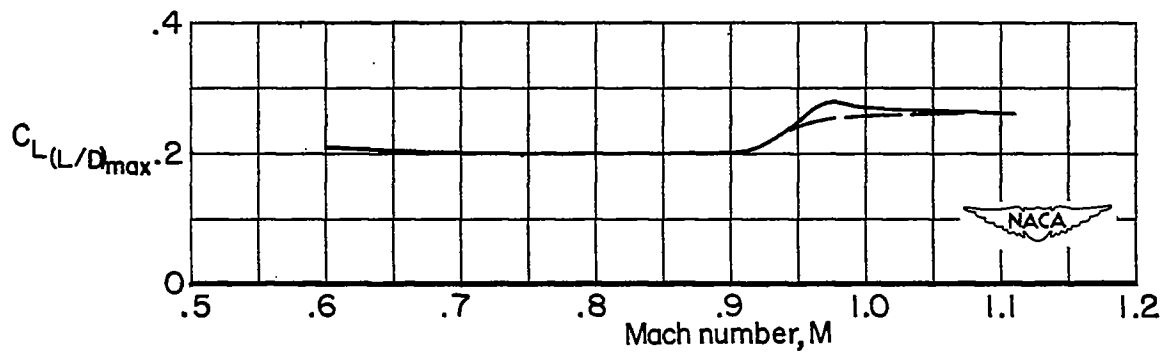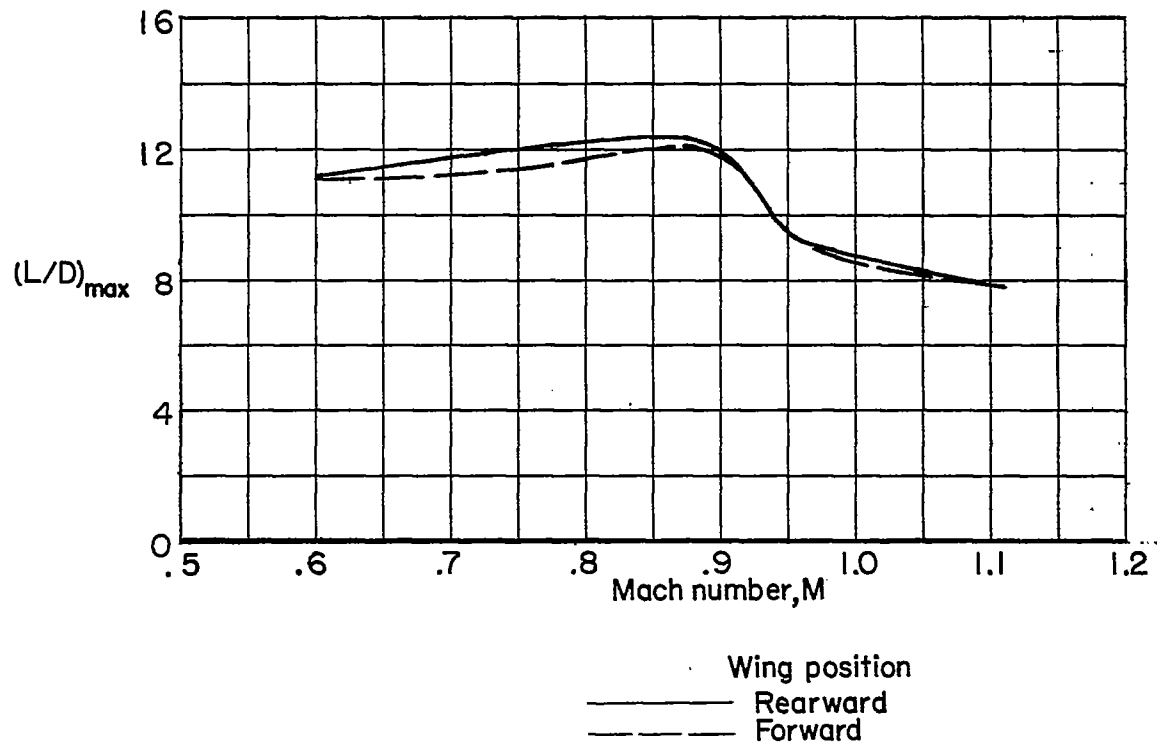
Figure 11.- Variation with Mach number of maximum lift-drag ratio and lift coefficient for the maximum lift-drag ratio for the unswept-wing—fuselage combinations.